

Nonlinear evolution of EMIC waves in a uniform magnetic field:

1. Hybrid simulations

N. Omidi,¹ R. M. Thorne,² and J. Bortnik²

Received 27 April 2010; revised 29 July 2010; accepted 20 October 2010; published 18 December 2010.

[1] We employ 2.5-D electromagnetic, hybrid simulations that treat ions kinetically via particle-in-cell methods and electrons as a massless fluid to study the long-term (hours) nonlinear evolution of electromagnetic ion cyclotron waves in the presence of multiple ion species in the outer magnetosphere. The source of the instability is a small population of hot (few keV) protons, representing plasma sheet ions at $L = 9$ with perpendicular temperature four times the parallel. In addition to the background population of cold protons the presence of minority, cold and heavy ions such as helium are also included. Both local (homogeneous) and nonlocal (finite-sized source region) simulations with uniform magnetic field have been carried out. In the case of a homogeneous system, parallel propagating ion cyclotron waves are generated with amplitudes of a few percent of the background magnetic field (a few nT). After about 1000 ion gyroperiods (~ 4 min) the wave amplitudes decrease by about 50% and remain nearly constant thereafter. The nonlinear evolution of the waves is associated with the gyrophase bunching of the cold protons and helium ions and reduction in the temperature anisotropy of the hot protons. In addition, parallel electrostatic waves with a wavelength half of that of the ion cyclotron waves are generated. These waves are subsequently absorbed and result in parallel heating of the cold ions. Throughout the run, both cold protons and heavy ions continue to gain energy primarily in the perpendicular direction while the hot protons reach isotropy followed by cooling in both parallel and perpendicular directions. In effect, the ion cyclotron waves continue to facilitate transfer of energy from the hot to cold ions. The results of simulations with localized hot protons show the simultaneous generation of ion cyclotron waves and expansion of the source region along the magnetic field. The nonlinear evolution of the waves is found to be similar to that seen in the homogeneous runs.

Citation: Omidi, N., R. M. Thorne, and J. Bortnik (2010), Nonlinear evolution of EMIC waves in a uniform magnetic field: 1. Hybrid simulations, *J. Geophys. Res.*, 115, A12241, doi:10.1029/2010JA015607.

1. Introduction

[2] Although, charge exchange and Coulomb scattering have been identified as the major loss processes responsible for the decay of the ring current during the recovery phase of the storm, evidence for removal of particles from the ring current on much shorter time scales (approximately an hour) during the main phase of the storm also exists [Gonzalez *et al.*, 1989; Prigancová and Feldstein, 1992; Feldstein *et al.*, 1994]. This faster ion precipitation is believed to be due to wave-particle interactions such as excitation and nonlinear evolution of electromagnetic ion cyclotron (EMIC) waves [e.g., Cornwall *et al.*, 1970; Anderson *et al.*, 1992a, 1992b; Thorne and Horne, 1997]. The most intense EMIC waves

are typically observed in association with elevated geomagnetic activity [Bräysy *et al.*, 1998; Erlandson and Ukhorskiy, 2001], and are found in the midnight-dusk region [Erlandson and Ukhorskiy, 2001; Fraser and Nguyen, 2001] but also in the dayside magnetosphere as far out as the magnetopause [e.g., Anderson *et al.*, 1992a, 1992b]. Typical amplitudes of EMIC waves in the magnetosphere, are of the order of a few nT and rank among the largest of all magnetospheric electromagnetic waves [Fraser *et al.*, 1996; Erlandson and Ukhorskiy, 2001; Fraser and Nguyen, 2001].

[3] The importance of EMIC waves in ion precipitation and loss of ring current population has been demonstrated by global modeling studies [Kozyra *et al.*, 1997; Jordanova *et al.*, 1998, 2001, 2003; Jordanova, 2005; Khazanov *et al.*, 2002, 2006, 2007]. These models have been developed to understand the complex dynamical processes involved in ion injection, intensification of the ring current during the growth phase and its decay due to wave-particle interactions, charge exchange and Coulomb collisions. In order to follow the evolution of the system over long periods of time

¹Solana Scientific Inc., Solana Beach, California, USA.

²Department of Atmospheric and Oceanic Sciences, University of California, Los Angeles, California, USA.

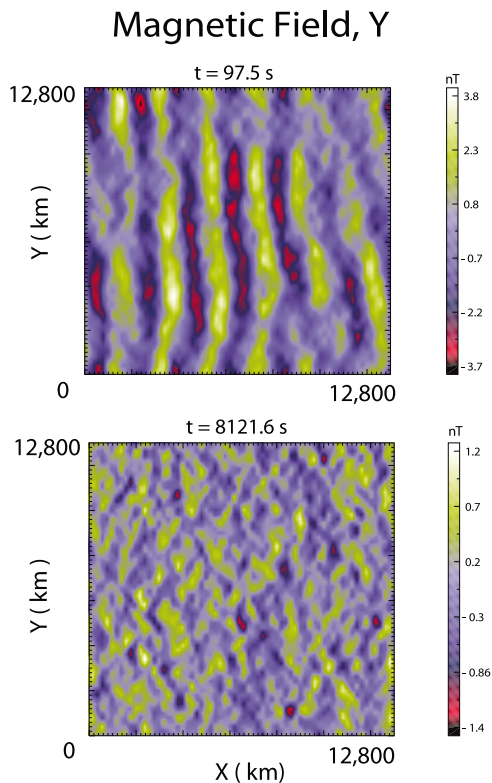


Figure 1. (top) B_y at a time when parallel ion cyclotron waves have maximum amplitude. (bottom) B_y at the end of the run when the waves have a smaller amplitude and propagate at oblique angles as well as parallel.

(i.e., days), these models use approximations such as bounce averaging (along the field line) of the particle motion in the magnetosphere and utilization of quasi-linear theory. In addition to causing ion precipitation, EMIC waves contribute to heating and acceleration of ionospheric ions in the magnetosphere [Thorne and Horne, 1997], and Landau resonant heating of thermal electrons [Cornwall et al., 1971; Thorne and Horne, 1992]. They also lead to resonant scattering and ultimate precipitation loss of relativistic outer zone electrons [Thorne and Kennel, 1971; Lyons and Thorne, 1972; Summers and Thorne, 2003; Meredith et al., 2003; Bortnik et al., 2006].

[4] EMIC waves are thought to be generated by an instability associated with the temperature anisotropy of ions with perpendicular temperature larger than parallel. The linear properties of this instability in a proton, electron plasma are reviewed by Gary [1993]. In the magnetosphere the generation and properties of EMIC waves are influenced by the presence of multiple populations and species of ions. Specifically, the source of the instability is the energetic ring current or plasma sheet proton population whose density is a few percent of the total plasma density. The remaining plasma in the outer magnetosphere consists mostly of cold protons and minority populations of heavier ions such as He^+ or O^+ . The presence of multiple ion species modifies the dispersive properties of EMIC waves and thus they occur in distinct frequency bands between the multiion

gyrofrequencies. The dispersion relation, and hence propagation characteristics (e.g., phase velocity) are dependent upon the relative concentrations of the various heavy ion species. These ions also affect reflection of the EMIC waves in the inner magnetosphere, and the coupling between the left- and right-hand polarized modes. In addition to affecting the linear properties of EMIC waves, the presence of heavy ions can lead to generation or suppression of wave growth in certain bands due to nonlinear wave-particle interactions [e.g., Thorne and Horne, 1997].

[5] In addition to quasi-linear theory, 1.5-D electromagnetic hybrid (kinetic ions, fluid electrons) simulations have been carried out in the past to examine the nonlinear evolution of EMIC waves [Omura et al., 1985; Denton et al., 1993; Gary and Lee, 1994; Gary et al., 1994]. These studies concentrated on the evolution of the system in the first few hundred to about thousand proton gyroperiods and showed the reduction in the temperature anisotropy of the energetic ions as well as heating of the helium ions. Recently, Hu and Denton [2009] have used 2.5-D hybrid simulations in a dipolar field to study the propagation and nonlinear evolution of EMIC waves. They show wave generation in the equatorial region and propagation to higher latitudes which is also associated with refraction of the waves and change from circular to linear polarization. This approach is highly useful and will pave the way to a much better understanding of EMIC waves and their role in particle dynamics in the inner magnetosphere. However, a number of questions related to the evolution of EMIC waves in a uniform magnetic field remain to be addressed as discussed here.

[6] The objective of this and the accompanying paper by Bortnik et al. [2010] is to further examine the nonlinear evolution of EMIC waves in a uniform magnetic field using 2.5-D hybrid simulations along with detailed test particle calculations that shed further light on the nature of wave particle interactions. As we show here, the nonlinear evolution of EMIC waves involves generation of electrostatic waves not discussed in the previous investigations. Similarly, we show that EMIC wave amplitudes remain substantial and result in heating of the cold ions (protons and He^+) for time periods much longer than that considered in the past studies. To achieve our objective, we have carried out a large number of simulations with different densities and levels of anisotropy of the hot protons. In this paper, we examine in some detail the nonlinear evolution of the instability for the case of 6% hot protons with perpendicular temperature 4 times larger than parallel temperature. These plasma parameters are suitable for dawn side magnetosphere at $L = 9$ as discussed by Horne and Thorne [1997]. Details regarding the scaling properties of the instability with density and level of temperature anisotropy of the hot protons are discussed in a forthcoming paper by J. Bortnik et al. (Parametric dependence of electromagnetic ion cyclotron wave saturation amplitudes, submitted to *Journal of Geophysical Research*, 2010). After describing the hybrid simulation model in section 2 we show results from the homogeneous simulations in section 3. In section 4 we show results from a simulation in which the source region (where hot ions exist) is confined to a portion of the simulation domain. Summary of the results and their implications for the impact of ion cyclotron waves in the magnetosphere and other space

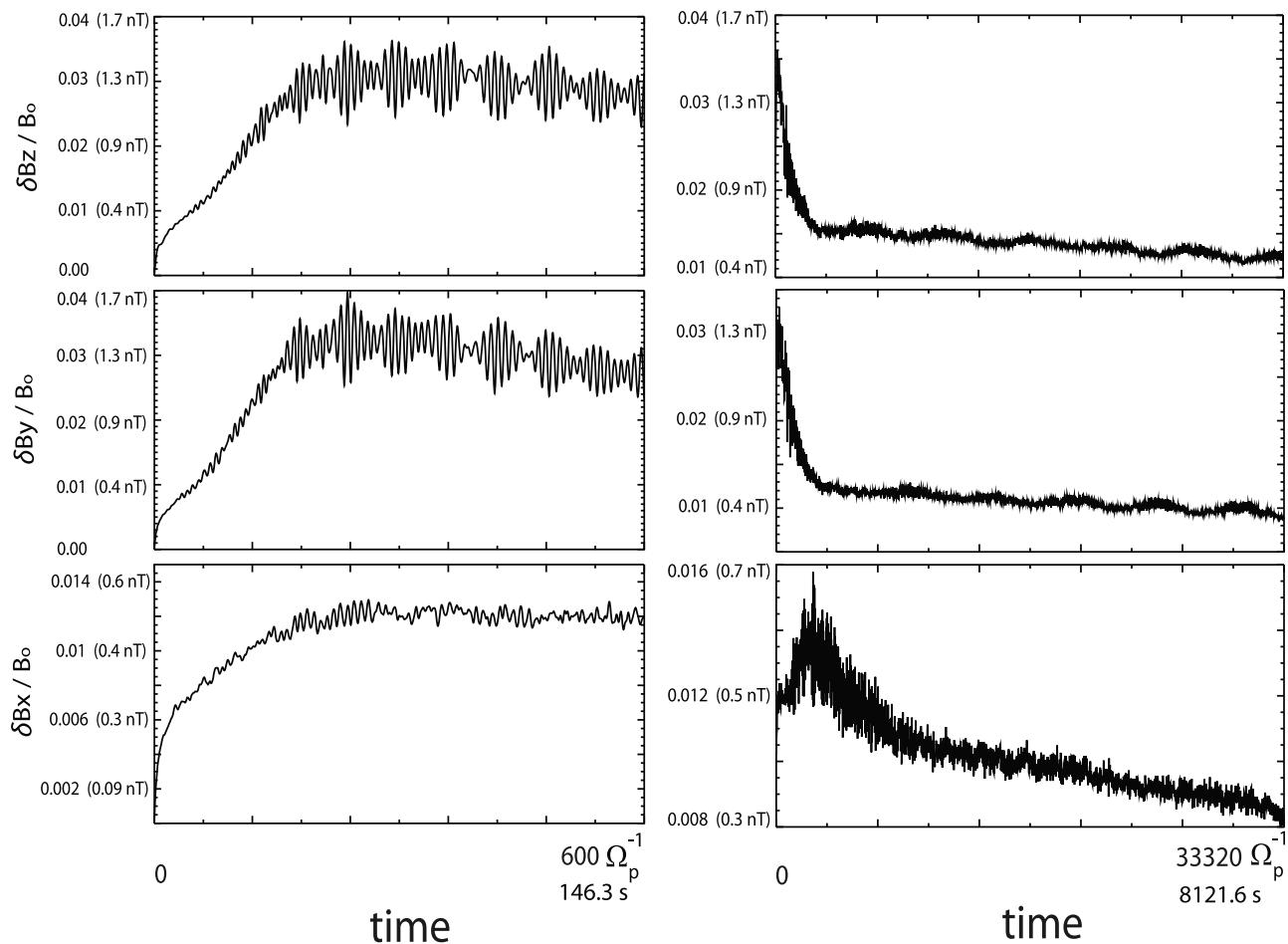


Figure 2. Time evolution of transverse and compressional field fluctuations. (left) Panels show early evolution of the waves; (right) panels correspond to the whole run.

plasma settings such as in the solar wind are provided in section 5.

2. Hybrid Simulation Model

[7] The main tools of investigation in this study are 2.5-D local and nonlocal hybrid simulations. The 2.5-D nature of the simulations implies that while the electromagnetic fields, currents and ion velocities are 3-D, only variations in 2 spatial dimensions (simulation plane, X and Y) are allowed and $\partial/\partial Z = 0$. In electromagnetic hybrid codes, ions are treated as macroparticles and consist of one or more species (e.g., differing mass, charge, etc.) whereas electrons are treated as a massless, charge neutralizing fluid [see, e.g., Winske and Omidi, 1993, 1996; Winske et al., 2003]. Hybrid codes are suited for physical phenomena that occur on ion time and spatial scales and where a kinetic description of the electrons is not required. The four equations that are solved include the Ampere's law without the displacement current (called the Darwin approximation) so that high-frequency light waves are eliminated. The second equation is the Faraday's law while the third is the electron momentum equation with electron mass equal to zero. This leads to the generalized Ohm's law that includes electron pressure gradients. The fourth equation is the Lorentz force law that

governs the motion of the ions. Standard particle-in-cell (PIC) methods are used to advance the ions. Note that due to the assumption of charge neutrality, Poisson's equation is not included.

[8] The spatial domain is covered by a rectilinear grid on which the electromagnetic field equations are solved. The electric and magnetic fields are used to compute the force on each ion which is then used to advance its velocity and position by a time step Δt , which is a small fraction of the ion gyroperiod. The positions and velocities of the ions are then recollected on the grid to update the ion density and current. The magnetic field is advanced in time from Faraday's law and the electric field is computed from the electron momentum equation. The assumption of charge neutrality implies that electrostatic waves with wavelengths of the order of or smaller than a Debye length are excluded from the model. However, as we show here long-wavelength electrostatic waves such as those associated with pressure gradients (and not charge separation) are accounted for in the model. We note that in some studies involving hybrid simulations [e.g., Hu and Denton, 2009], the electron pressure gradient term in the Ohm's law is not included and therefore, electrostatic waves are excluded. The electron current is related to the ion current and magnetic field by the Ampere's law. The electron pressure is typically determined

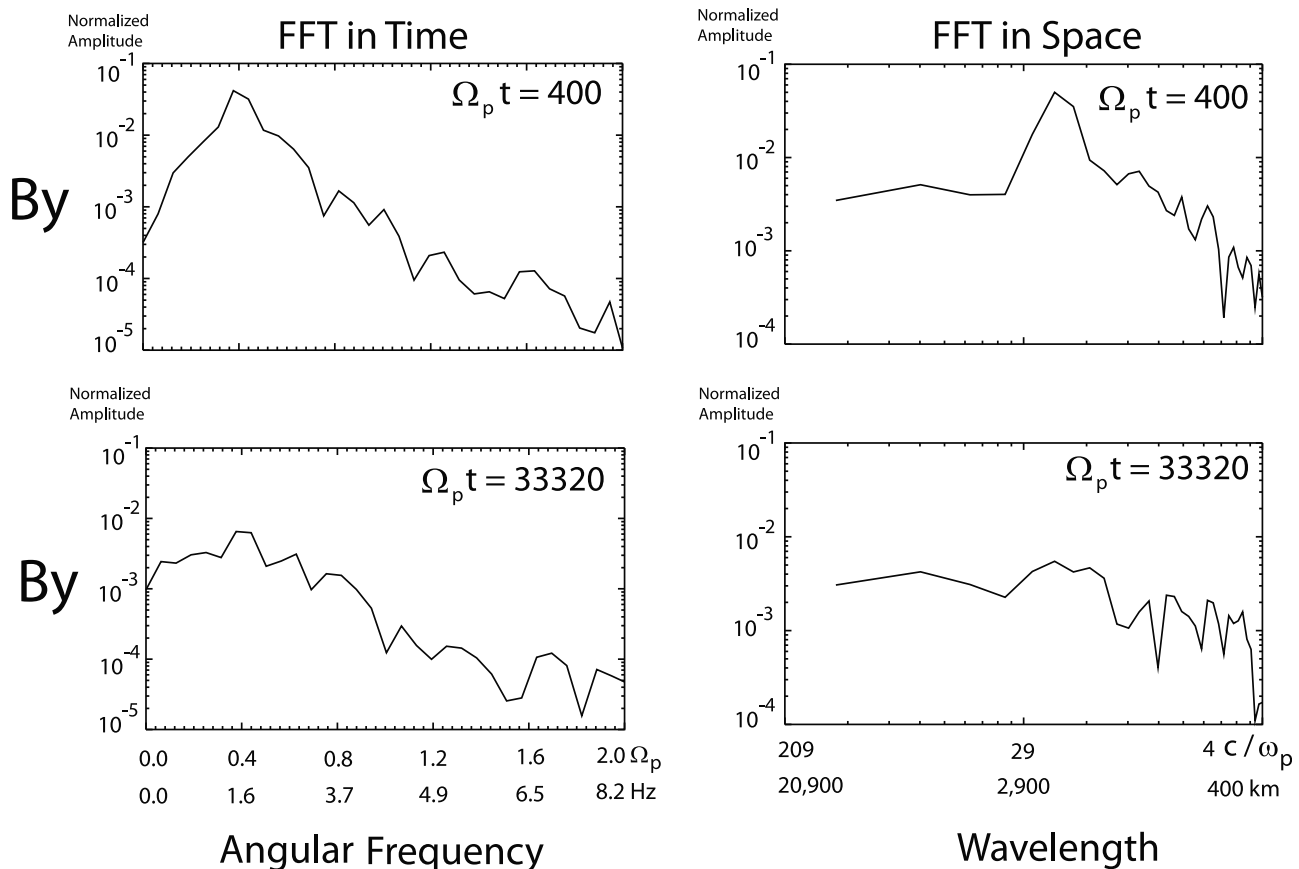


Figure 3. Results of FFT in (left) time and (right) space at the same two times as in Figure 1. The time window length is 50 proton gyroperiods. See text for more details.

by an equation of state and here we assume an isothermal model.

[9] In the local simulations we assume spatial homogeneity and use doubly periodic boundary conditions. Subsequently, in the nonlocal simulations, the energetic protons are confined in the X (magnetic field) direction and placed in the middle of the box. This allows for waves to be generated in the middle of the box and propagate out in both +X and -X directions and mimics wave generation in the equatorial regions and propagation to higher latitudes before magnetic field gradients become significant. Periodic boundary conditions are used in Y direction.

[10] The local simulation box lies in the X-Y plane and extends 128 proton skin depths c/ω_p , where c is the speed of light and ω_p is the ion plasma frequency (12,800 km) in X and Y directions. Cell size of 2×2 proton skin depth is used with 64 macroparticles per cell for each ion population or species. The plasma parameters used in this study are similar to those used by *Horne and Thorne* [1997] and typical of those observed by *Anderson et al.* [1996]. The plasma consists of 6% hot (plasma sheet) protons with parallel temperature of 1.3 keV and perpendicular temperature 4 times the parallel temperature. Cold protons with parallel temperature of 30 eV and perpendicular energy of 10 eV constitute the majority of ions, while 0.8% He^+ ions with parallel temperature of 20 eV and perpendicular energy of 3 eV are also present. The electrons have parallel and perpendicular temperatures of 0.01 eV. We use total density

of 5 cm^{-3} and magnetic field of 43 nT to simulate EMIC generation in the dayside magnetosphere near $L = 9$ field line.

[11] In the nonlocal simulations, the box extends 3600 proton skin depth (360,000 km) in the X direction and 360 proton skin depth in Y. The hot protons are initially localized in the region $1700 < X < 1900$ while cold protons are present throughout the box. The density of the hot protons corresponds to 6% and their perpendicular temperature is 4 times the parallel temperature.

3. Results From Local Simulations

[12] Figure 1 shows the transverse (Y) component of the magnetic field at a relatively early time ($400 \Omega_p^{-1}$ where Ω_p is the proton angular gyrofrequency which for 43 nT field corresponds to 4.1 Hz) and at the end of the simulation ($33320 \Omega_p^{-1}$, 8121.6 s) in the X-Y plane. The phase fronts seen in Figure 1 (top) correspond to ion cyclotron waves generated with wave vectors primarily along the magnetic field propagating in both +X and -X directions as expected from linear theory. Figure 1 (bottom) demonstrates less coherent wavefronts associated with waves propagating along and oblique to the magnetic field and smaller amplitudes.

[13] Figure 2 shows the time evolution of the spatially averaged (over the entire simulation box) amplitude of the transverse (top two panels) and compressional field fluctuations normalized to the background magnetic field. Figure 2

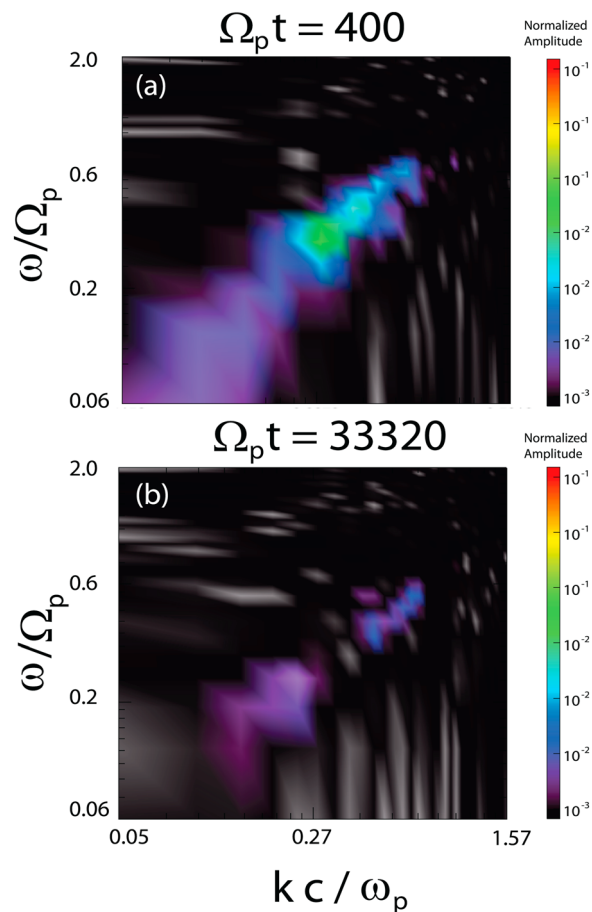


Figure 4. Amplitude spectrums in ω - k space at the same two times as in Figure 1. They demonstrate that waves are on ion cyclotron branch during saturation and the end of the run. See text for more details.

(left) corresponds to the first 600 proton gyroperiods (146.3 s) in the run and shows the growth of the waves and saturation where the amplitudes remain nearly constant. As expected, the waves are primarily transverse and circularly polarized ($\partial B_y \sim \partial B_z > \partial B_x$). The initial noise level in the simulations corresponds to amplitudes of $\sim 10^{-4}$ times the background magnetic field (0.0043 nT). This implies that wave saturation occurs at ~ 6 e-foldings. Figure 2 (right) corresponds to the entire duration of the run and shows that after a few 1000 proton gyroperiods (~ 4 min) the transverse wave amplitudes decrease by about 50% and remain nearly constant thereafter.

[14] To further examine the properties of the waves, Figures 3 (left) and 3 (right) show the result of FFT in time and space, respectively. For FFT in time we use a time window length of 50 gyroperiods and the entire length (in X) of the simulation box is used for FFT in space. The FFT results at $\Omega_p t = 400$ (97.5 s) show maximum amplitude (normalized to background magnetic field) at frequencies ~ 1.6 He^+ gyrofrequency (1.6 Hz) and wave number around 0.22 inverse inertial length (wavelength of ~ 2500 km) which agree well with the results of linear theory presented by *Horne and Thorne* [1997]. At the end of the run (bottom panels) the amplitudes are smaller and the spectrum is broader in both frequency and wave number but still shows maximum

power at the same frequency. To illustrate the dispersive properties of the waves, Figure 4 shows the amplitude spectrum in ω - k space at $\Omega_p t = 400$ and 33320. Power falls on the ion cyclotron branch both at early times and the end of the simulation illustrating that no other electromagnetic branches are excited as a result of the nonlinear evolution of the waves.

[15] Figure 5 shows the time evolution of the perpendicular and parallel energies of the hot protons normalized to their initial values with Figure 5 (left) corresponding to the first 600 proton gyroperiods (146.3 s) and Figure 5 (right) covering the entire simulation time (8121.6 s). As can be seen, during the first ~ 6600 proton gyroperiods (1600 s) the perpendicular energy of the protons decreases with time while the parallel energy increases until they reach isotropy. Subsequently, both perpendicular and parallel energies decrease with time at nearly equal rates.

[16] Figures 6 and 7 show the time evolution of the cold protons and He^+ ions, respectively, in the same format as in Figure 5. They show that both ion species gain energy in time and mostly in the perpendicular directions. In both cases the rate of acceleration decreases after ~ 1000 proton gyroperiods (4 min) but continues throughout the run. Although when normalized to their initial energies, the He^+ ions apparently gain a lot more energy than the cold protons, when the difference in their densities is taken into account the two species gain similar levels of energy and develop similar levels of temperature anisotropies by the end of the run. The details of the particle acceleration process have been investigated using test particle calculations and are discussed by *Bortnik et al.* [2010].

[17] To illustrate the effects of EMIC waves on the He^+ ions, Figure 8 shows their phase space density plot at $\Omega_p t = 400$ (97.5 s). This plot shows the gyrophase angle and position in X of each ion where gyrophase angle corresponds to the angle between the perpendicular velocity of the particle and the y axis. It is evident that the ions are well organized in phase space due to interaction with the EMIC waves. This organization can be described as a series of striations belonging to two classes where in one the gyrophase increases with X and in the other it decreases. The dashed red lines shown in Figure 8 are drawn to help with identification of these two families of striations. This behavior is consistent with gyrophase bunching of the ions by ion cyclotron waves propagating parallel and antiparallel to the magnetic field that despite similar polarizations have opposite helicities (sense of rotation of the transverse field in space). We note that spacecraft observations of the modulations of He^+ fluxes by EMIC waves led to the suggestion that these ions are gyrophase trapped by the waves [e.g., *Mauk et al.*, 1981; *Roux et al.*, 1982; *Berchem and Gendrin*, 1985]. The results shown here and in the companion paper by *Bortnik et al.* [2010] provide further support for this interpretation.

[18] The gyrophase bunching of ions by the waves propagating parallel and antiparallel to the magnetic field leads to an interesting physical process that does not occur when only one wave is present in the system. As illustrated in Figure 8, each striation with a given helicity intersects two striations with the opposite helicity. Since at these points/regions of intersection more ions are present, densities are higher leading to spatial fluctuations in ion density. Because each striation intersects two striations with the opposite

Hot Protons

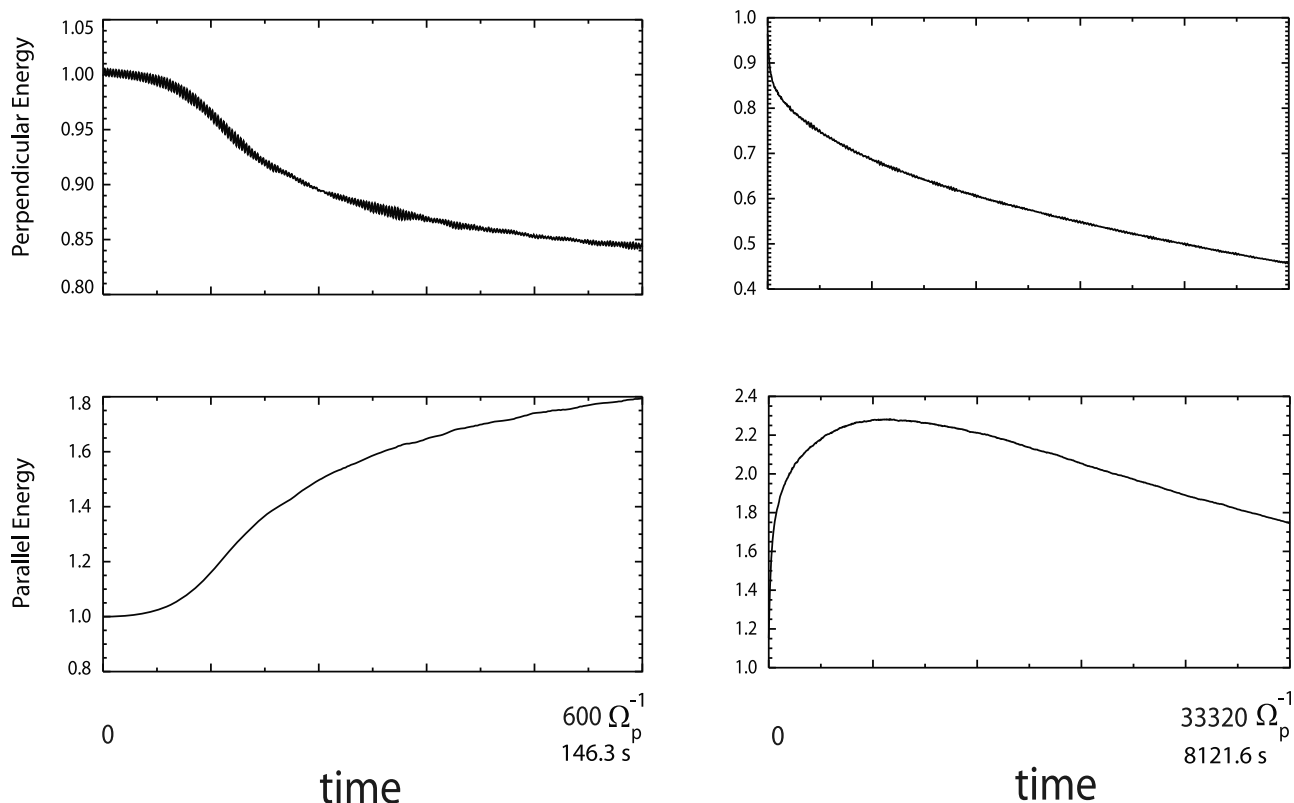


Figure 5. The time evolution of parallel and perpendicular energies of hot protons normalized to their initial values. (left) Panels show early evolution of the hot protons; (right) panels correspond to the whole run.

helicity the wavelength of the density fluctuations is half of that of the EMIC waves. The oscillations in helium density due to this process are shown in Figure 9 (top). These density oscillations also imply pressure fluctuations with gradients in the X direction that in turn result in fluctuating parallel electric fields. These waves are shown in Figure 9 (bottom). As expected the wavelength of these fluctuations is also half that of the EMIC waves.

[19] Generation of field aligned electrostatic waves through nonlinear coupling of oppositely propagating ion cyclotron waves results in parallel heating of the cold ions. Examination of the $V_x - X$ phase space (not shown here), shows clear evidence for the trapping and heating of He^+ ions by the electrostatic waves. These waves get mostly damped by $\Omega_p t \sim 1000$ (4 min) by which time the level of gyrophase bunching of the cold ions also reduces considerably. It should be noted that the effects of EMIC waves on the cold protons are very similar to He^+ ions in that they also are gyrophase bunched in space and are associated with density fluctuations with wavelength half of the EMIC waves. In contrast, the density of the hot protons shows no sign of such fluctuations. As shown by *Bortnik et al.* [2010], EMIC waves result in gyrophase trapping of some resonant hot ions. However, this trapping is not sufficient to result in any spatial organization such as those seen for the cold ions (e.g., Figure 8) where in

contrast the whole population is trapped and gyrophase bunched.

[20] We note that although gyrophase bunching of cold ions and the resulting electrostatic waves occur over a wide range of parameters, when the hot ion density or temperature anisotropy are small and the instability is weak they are not a part of the saturation processes. Either way, however, the wave saturation amplitudes remain appreciable over a long time and cold ions are accelerated in the perpendicular and lesser degree parallel directions. The parametric dependencies of the saturation process are discussed in detail by *Bortnik et al.* (submitted manuscript, 2010).

4. Nonlocal Simulations

[21] The results from local hybrid simulations provide us with a basic understanding of the nonlinear processes associated with the evolution of EMIC waves. The next step toward understanding of the evolution and impacts of the EMIC waves in the magnetosphere is to consider the impacts of spatial inhomogeneities in plasma and magnetic field. In this section we examine the effects of the finite size of the region where hot ions are present as is the case in the magnetosphere where the plasma sheet ions are confined to low-latitude regions. We note that the size of the simulation box in

Cold Protons

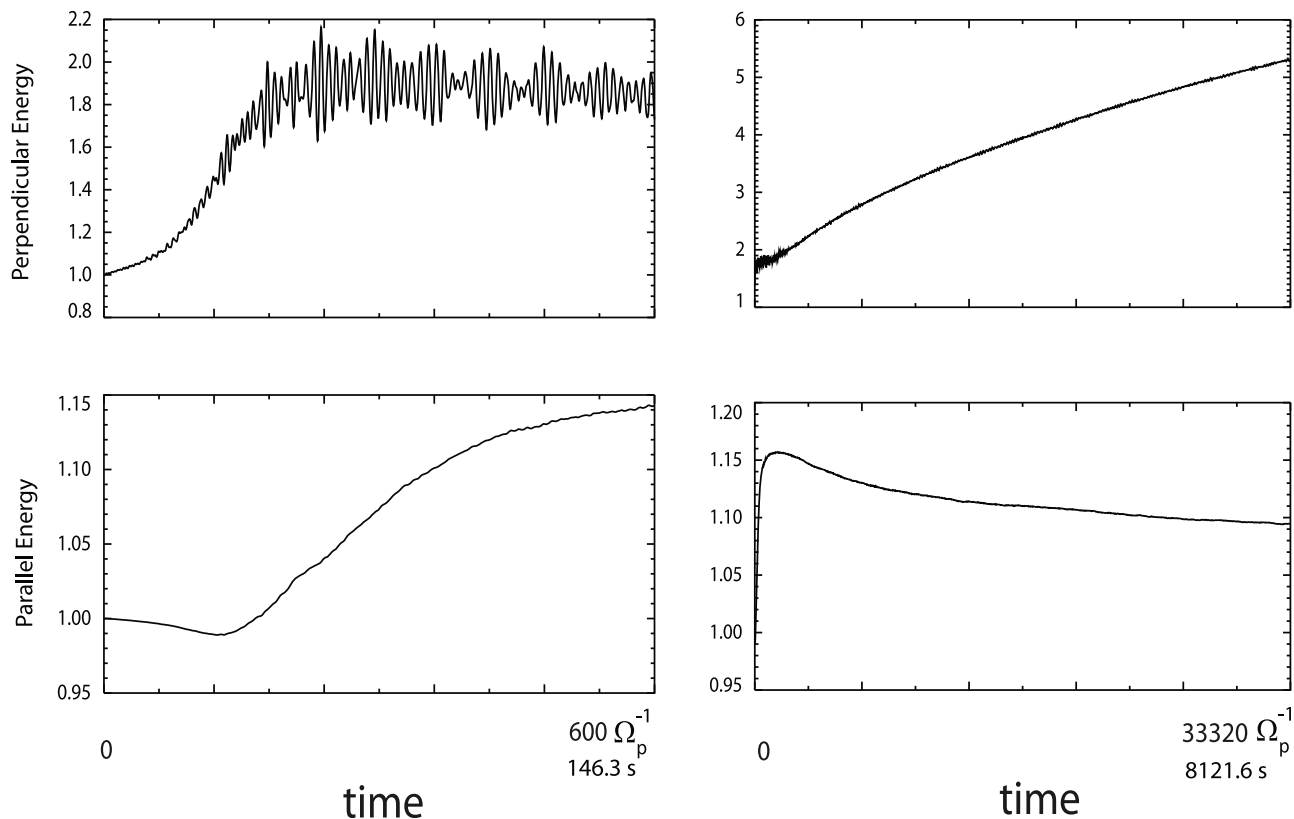


Figure 6. Time evolution of parallel and perpendicular energies of the cold protons. (left) Panels show early evolution of the cold protons; (right) panels correspond to the whole run.

the X direction is taken to be large enough (360,000 km) to allow for the run to continue for at least 1000 gyroperiods before the hot ions and EMIC waves reach the left and right hand boundaries. In the magnetosphere, magnetic field gradients occur on smaller scales and the assumption of a uniform field for such distances is not valid.

[22] Figure 10 shows the result from a run where the hot ions are initially loaded in the region $1700 < X < 1900$ with plasma parameters similar to the initial conditions in section 3 (at time 1000 gyroperiods, 4 min). Figure 10 (top) shows the Z component of the magnetic field and illustrates the presence of transverse fluctuations in the region $1000 < X < 2600$ due to generation and propagation of EMIC waves. Figure 10 (middle) shows the Poynting vector with positive values (green and white colors) indicating propagation in the X direction and negative values (blue and red) in the $-X$ direction. Figure 10 (bottom) shows the density of the hot ions which by this time in the simulation have expanded to the region $200 < X < 3400$. This expansion occurs as a result of the uninhibited motion of the ions along the magnetic field as well as pitch angle scattering by the EMIC waves.

[23] Given that the hot ions have expanded to such a large region, the question that arises is the extent of the region where wave generation is taking place. Examination of the Poynting vector shows mixed polarity (i.e., positive and negative) in the region $1400 < X < 2200$ indicating the

presence of waves propagating parallel and antiparallel to the magnetic field. On the other hand, the Poynting vector is primarily negative for $X < 1400$ and positive for $X > 2200$. This suggests that the region of wave generation where one expects the presence of waves propagating in both directions has expanded to $1400 < X < 2200$ which represents an increase by a factor of 4 compared to the original width of the hot ions.

[24] Figure 11 shows, from top to bottom, the density of the hot protons, the Poynting vector, the X component of the electric field, and the Z component of the magnetic field along a cut in the X direction and $Y = 18,000$ km. It is evident that because of their expansion along the field the local density of the hot ions is considerably below the original 6%. Using the lower densities of the hot protons at later times would suggest that the instability is too weak for gyrophase bunching of ions and generation of electrostatic waves. However, we can determine that the nonlinear evolution of the system is in fact consistent with expectations based on the initial density of the hot ions by noting the presence of E_x fluctuations associated with the generation of field aligned electrostatic waves. Although hard to see in Figure 11, the wavelength of these waves is half that of the EMIC waves as expected. The fact that the initial value of hot ion density determines the nonlinear evolution of the instability is tied to the fact that the reduction in density of hot ions takes place at later times when the waves have grown in amplitude and

Helium

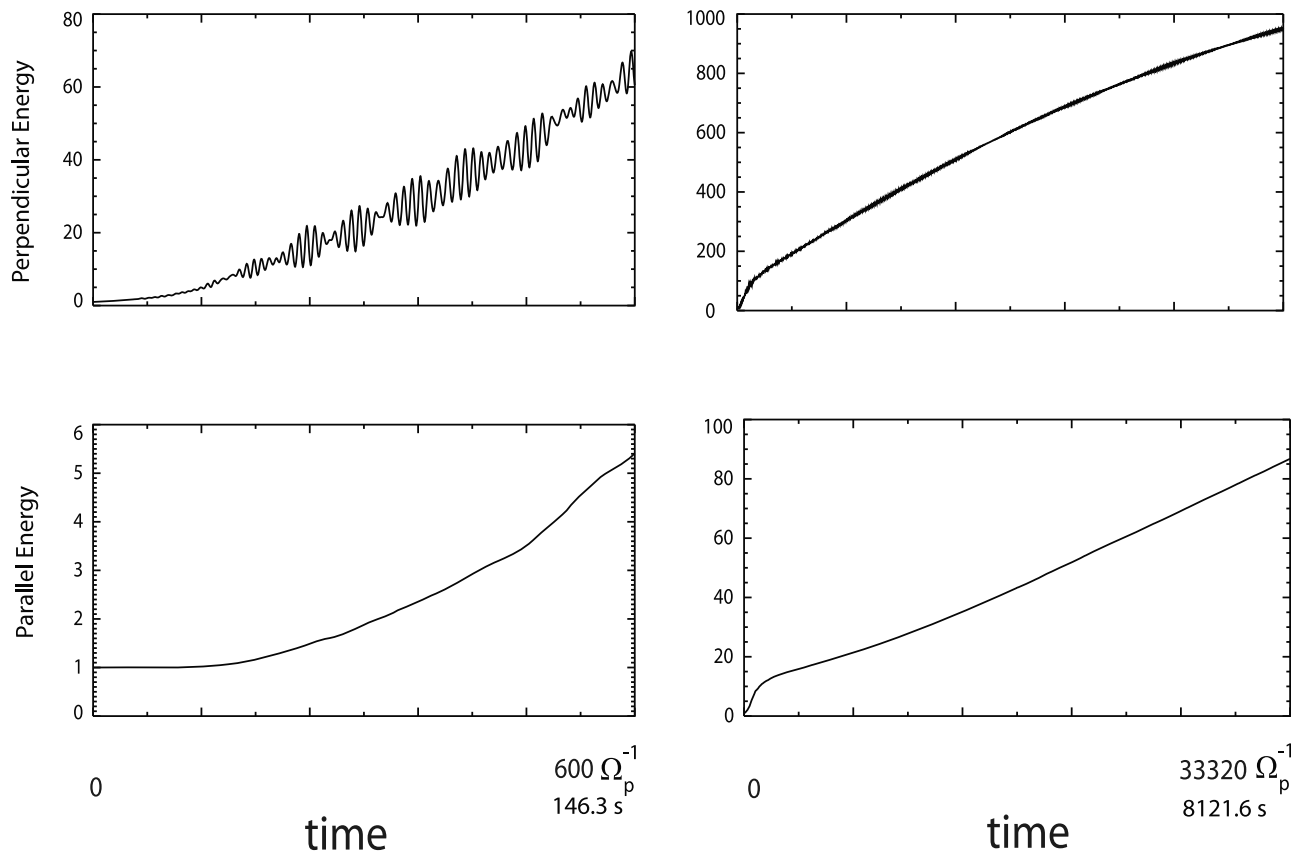


Figure 7. Time evolution of parallel and perpendicular energies of He^+ ions. (left) Panels show early evolution of the He^+ ions; (right) panels correspond to the whole run.

one is not starting with amplification of waves at the noise level. In other words the expansion of the hot ions and evolution of the instability are a tightly coupled process and cannot be viewed as a simple expansion followed by wave generation.

5. Summary and Conclusions

[25] In this paper we showed results from local and non-local electromagnetic hybrid simulations to describe the long-term, nonlinear evolution of EMIC waves. During the first ~ 1000 proton gyroperiods (4 min) the wave amplitudes grow to a few percent of the background magnetic field level (a few nT) and stay nearly constant thereafter. In this stage of the instability both cold protons and the He^+ ions are gyrophase bunched in space by the EMIC waves propagating parallel and antiparallel to the magnetic field. The gyrophase bunching of He^+ ions is consistent with the observed modulations of He^+ fluxes by the EMIC waves in spacecraft data which was interpreted as evidence of gyrophase bunching by *Mauk et al.* [1981], *Roux et al.* [1982], and *Berchem and Gendrin* [1985].

[26] It was demonstrated in this paper that the gyrophase bunching of the cold ions by the waves propagating in both directions along the magnetic field is associated with the

generation of parallel electrostatic waves with a wavelength half of that of the EMIC waves. Therefore, it is essential that hybrid simulation studies of EMIC waves include the electron pressure gradient term in the generalized Ohm's law in order for the electrostatic waves to be included in the model.

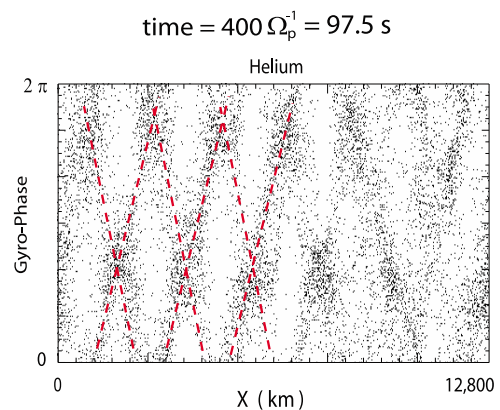


Figure 8. Phase space plot of He^+ ions showing their gyrophase bunching by waves propagating parallel and antiparallel to X.

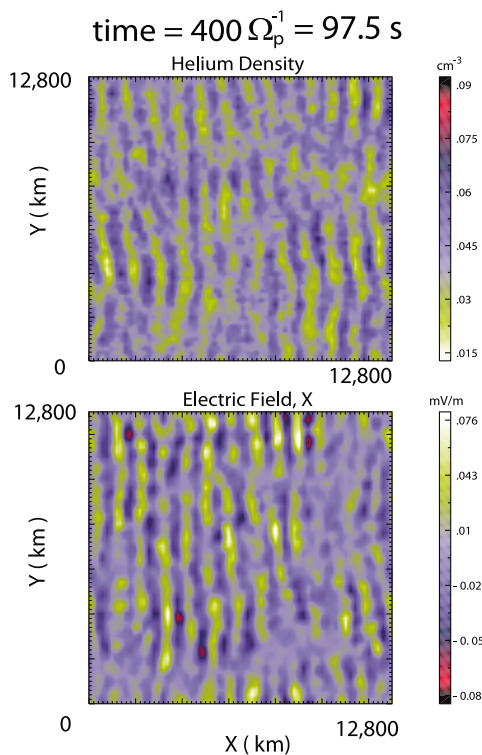


Figure 9. (top) Fluctuations in the density of He^+ ions and (bottom) the X component of the electric field associated with the nonlinearly generated electrostatic waves with wavelength half that of EMIC waves.

These waves are associated with the electrostatic trapping of the cold ions in the parallel direction resulting in their heating. After ~ 1000 gyroperiods (4 min), the transverse amplitudes decrease by $\sim 50\%$ while the field aligned electrostatic waves dissipate completely. Despite the drop to a lower level, the wave amplitude of the EMIC waves remain appreciable (a few % of the background, $\sim \text{nT}$) for many thousands of proton gyroperiods (hours). Spectral analysis of these waves shows that they remain on the ion cyclotron branch. The cold protons and He^+ ions gain energy throughout the run primarily in the perpendicular direction but also in the parallel direction. The details of this acceleration process are discussed by *Bortnik et al.* [2010]. Although when normalized to their initial energies the He^+ ions gain a larger fraction than the cold protons when the differences in their densities are taken into account cold protons gain little more energy. The hot ions are observed to become isotropic followed by loss of energy in both parallel and perpendicular directions.

[27] By performing nonlocal simulations with a finite size source region, we find that the expansion of the hot ions along the magnetic field results in considerable broadening of the wave generation region. Despite this expansion and reduction of the hot proton density, we showed that the nonlinear evolution of the instability is determined by the initial density of these ions. This illustrates the coupled nature of the expansion of the hot ions and wave generation processes. The results from nonlocal simulations show that the saturation mechanisms observed in the homogeneous system also operate in inhomogeneous systems. Thus, EMIC waves could be highly efficient in ion scattering and accel-

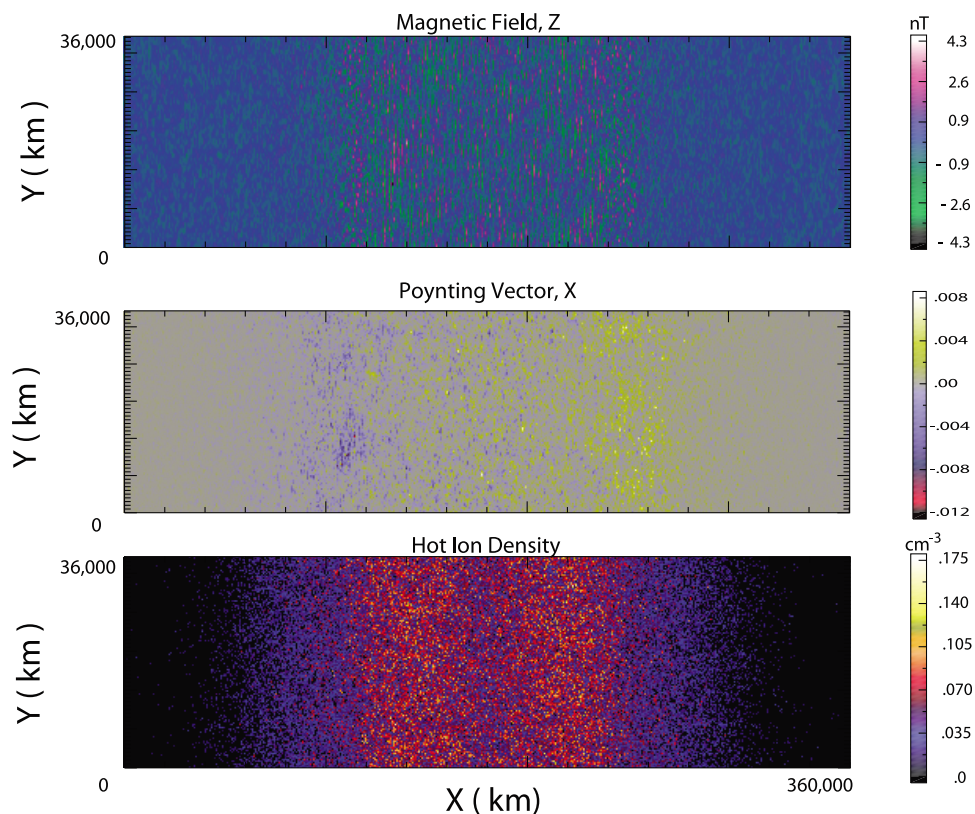


Figure 10. Plots of (top) wave amplitude, (middle) Poynting vector, and (bottom) hot ion density from a nonlocal run.

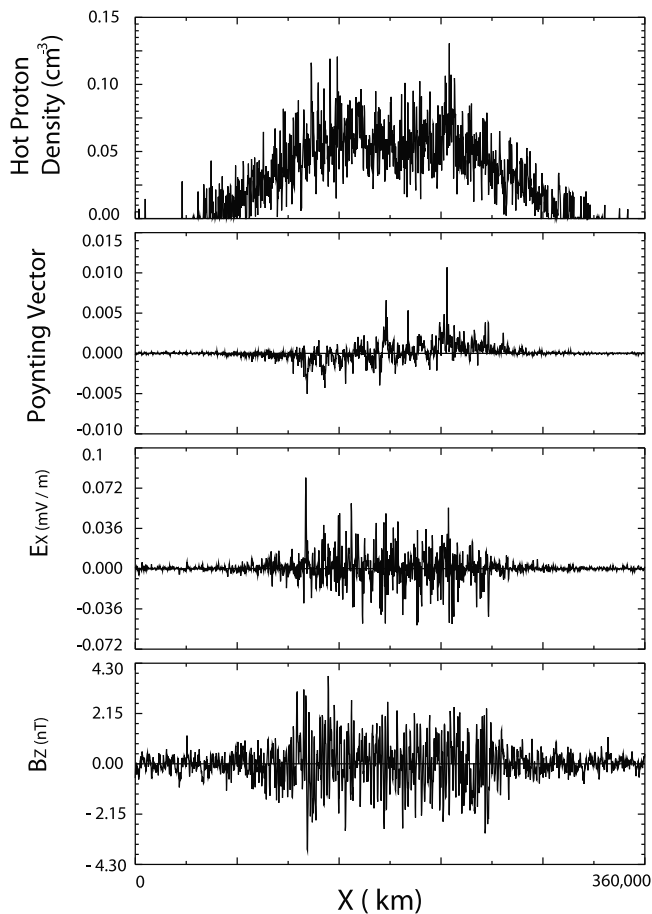


Figure 11. Variations along a cut in X direction. Shown is the generation of electrostatic waves similar to those seen in periodic simulations.

eration for very long periods of time (hours). In the case of the magnetosphere, the dipolar geometry of the magnetic field results in refraction of EMIC waves as they propagate to higher latitudes [e.g., *Horne and Thorne*, 1993, 1994; *Hu and Denton*, 2009]. As such, the results presented here are relevant up to the time when wave refraction becomes significant. Hybrid simulations with dipolar geometry have begun to address this important question [*Hu and Denton*, 2009] and we will be presenting results from such a model in the near future.

[28] There are, however, other space plasma settings where ion cyclotron waves are generated and can propagate for long distances in a nondipolar magnetic field. One such example is the observations of ion cyclotron waves in the solar wind. *Jian et al.* [2009] have found that narrow-band ion cyclotron waves are ubiquitous in the solar wind, far away from any planets and shocks. These waves often appear when the interplanetary magnetic field is more radial than the nominal Parker spiral. They propagate nearly parallel to the magnetic field and are below the local proton gyrofrequency in the solar wind frame. Because the wave frequency in the spacecraft frame is higher than the local proton gyrofrequency, the waves cannot be locally generated by the pickup ions. The observations are consistent with wave generation closer to the Sun and outward transport by the solar wind. These waves are intrinsically left-hand polarized

in the solar wind frame, and appear left- and right-handed in the spacecraft frame due to outward and inward propagation, respectively. These observations are consistent with the results presented here that ion cyclotron waves can persist for long times and propagate along the magnetic field long distances away from the initial source region.

[29] **Acknowledgments.** Work for this project was supported by NASA grant NNX08AM17G to Solana Scientific Inc.

[30] Robert Lysak thanks Colin Waters and the other reviewers for their assistance in evaluating this manuscript.

References

- Anderson, B. J., R. E. Erlandson, and L. J. Zanetti (1992a), A statistical study of Pc 1–2 magnetic pulsations in the equatorial magnetosphere: 1. Equatorial occurrence distribution, *J. Geophys. Res.*, *97*, 3075–3088, doi:10.1029/91JA02706.
- Anderson, B. J., R. E. Erlandson, and L. J. Zanetti (1992b), A statistical study of Pc 1–2 magnetic pulsations in the equatorial magnetosphere: 2. Wave properties, *J. Geophys. Res.*, *97*, 3089–3101, doi:10.1029/91JA02697.
- Anderson, B. J., R. E. Denton, G. Ho, D. C. Hamilton, S. A. Fuselier, and R. J. Strangeway (1996), Observational test of local proton cyclotron instability in the Earth's magnetosphere, *J. Geophys. Res.*, *101*, 21,527–21,543, doi:10.1029/96JA01251.
- Berchem, J., and R. Gendrin (1985), Nonresonant interaction of heavy ions with electromagnetic ion cyclotron waves, *J. Geophys. Res.*, *90*, 10,945–10,960, doi:10.1029/JA090iA11p10945.
- Bortnik, J., R. M. Thorne, T. P. O'Brien, J. C. Green, R. J. Strangeway, Y. Y. Shprits, and D. N. Baker (2006), Observation of two distinct, rapid loss mechanisms during the 20 November 2003 radiation belt dropout event, *J. Geophys. Res.*, *111*, A12216, doi:10.1029/2006JA011802.
- Bortnik, J., R. M. Thorne, and N. Omidi (2010), Nonlinear evolution of EMIC waves in a uniform magnetic field: 2. Test-particle scattering, *J. Geophys. Res.*, *115*, A12242, doi:10.1029/2010JA015603.
- Bräysy, T., K. Mursula, and G. Marklund (1998), Ion cyclotron waves during a great magnetic storm observed by Freja double-probe electric field instrument, *J. Geophys. Res.*, *103*(A3), 4145–4155, doi:10.1029/97JA02820.
- Cornwall, J. M., F. W. Coroniti, and R. M. Thorne (1970), Turbulence loss of ring current protons, *J. Geophys. Res.*, *75*, 4699–4709, doi:10.1029/JA075i025p04699.
- Cornwall, J. M., F. V. Coroniti, and R. M. Thorne (1971), Unified theory of SAR arc formation at the plasmopause, *J. Geophys. Res.*, *76*, 4428–4445, doi:10.1029/JA076i019p04428.
- Denton, R. E., M. K. Hudson, S. A. Fuselier, and B. J. Anderson (1993), Electromagnetic ion cyclotron waves in the plasma depletion layer, *J. Geophys. Res.*, *98*, 13,477–13,490, doi:10.1029/93JA00796.
- Erlandson, R. E., and A. J. Ukhorskiy (2001), Observations of electromagnetic ion cyclotron waves during geomagnetic storms: Wave occurrence and pitch angle scattering, *J. Geophys. Res.*, *106*, 3883–3895, doi:10.1029/2000JA000083.
- Feldstein, Y. I., et al. (1994), Ring current and auroral electrojet in conjunction with interplanetary medium parameters during magnetic storms, *Ann. Geophys.*, *12*, 602–611, doi:10.1007/s00585-994-0602-6.
- Fraser, B. J., and T. S. Nguyen (2001), Is the plasmopause a preferred region of electromagnetic ion cyclotron waves in the magnetosphere?, *J. Atmos. Sol. Terr. Phys.*, *63*, 1225–1247, doi:10.1016/S1364-6826(00)00225-X.
- Fraser, B. J., H. J. Singer, W. J. Hughes, J. R. Wygant, R. R. Anderson, and Y. D. Hu (1996), CRRES Poynting vector observations of electromagnetic ion cyclotron waves near the plasmopause, *J. Geophys. Res.*, *101*, 15,331–15,343, doi:10.1029/95JA03480.
- Gary, S. P. (1993), *Theory of Space Plasma Microinstabilities*, Cambridge Univ. Press, New York, doi:10.1017/CBO9780511551512.
- Gary, S. P., and M. A. Lee (1994), The ion cyclotron anisotropy instability and the inverse correlation between proton anisotropy and proton beta, *J. Geophys. Res.*, *99*, 11,297–11,301, doi:10.1029/94JA00253.
- Gary, S. P., M. E. McKean, D. Winske, B. J. Anderson, R. E. Denton, and S. A. Fuselier (1994), The proton cyclotron instability and the anisotropy β inverse correlation, *J. Geophys. Res.*, *99*, 5903–5914, doi:10.1029/93JA03583.
- Gonzalez, W. D., B. T. Tsurutani, A. L. C. Gonzalez, E. J. Smith, F. Tang, and S.-I. Akasofu (1989), Solar wind-magnetosphere coupling during

- intense magnetic storms (1978–1979), *J. Geophys. Res.*, *94*, 8835–8851, doi:10.1029/JA094iA07p08835.
- Horne, R. B., and R. M. Thorne (1993), On the preferred source location for the convective amplification of ion cyclotron waves, *J. Geophys. Res.*, *98*, 9233–9247, doi:10.1029/92JA02972.
- Horne, R. B., and R. M. Thorne (1994), Convective instabilities of electromagnetic ion cyclotron waves in the outer magnetosphere, *J. Geophys. Res.*, *99*, 17,259–17,273, doi:10.1029/94JA01259.
- Horne, R. B., and R. M. Thorne (1997), Wave heating of He⁺ by electromagnetic ion cyclotron waves in the magnetosphere: Heating near the H⁺-He⁺ bi-ion resonance frequency, *J. Geophys. Res.*, *102*, 11,457–11,471, doi:10.1029/97JA00749.
- Hu, Y., and R. E. Denton (2009), Two-dimensional hybrid code simulation of electromagnetic ion cyclotron waves in a dipole magnetic field, *J. Geophys. Res.*, *114*, A12217, doi:10.1029/2009JA014570.
- Jian, L. K., C. T. Russell, J. G. Luhmann, R. J. Strangeway, J. S. Leisner, and A. B. Galvin (2009), Ion cyclotron waves in the solar wind observed by STEREO near 1 AU, *Astrophys. J.*, *701*, L105–L109, doi:10.1088/0004-637X/701/2/L105.
- Jordanova, V. K. (2005), Sources, transport, and losses of energetic particles during geomagnetic storms, in *The Inner Magnetosphere: Physics and Modeling*, *Geophys. Monogr. Ser.*, vol. 155, edited by T. I. Pulkkinen, N. A. Tsyganenko, and R. H. W. Friedel, pp. 9–21, AGU, Washington, D. C.
- Jordanova, V. K., C. J. Farrugia, J. M. Quinn, R. M. Thorne, K. E. Ogilvie, R. P. Lepping, G. Lu, A. J. Lazarus, M. F. Thomsen, and R. D. Belian (1998), Effect of wave-particle interactions on ring current evolution for January 10–11, 1997: Initial results, *Geophys. Res. Lett.*, *25*, 2971–2974, doi:10.1029/98GL00649.
- Jordanova, V. K., C. J. Farrugia, R. M. Thorne, G. V. Khazanov, G. D. Reeves, and M. F. Thomsen (2001), Modeling ring current proton precipitation by EMIC waves during the May 14–16, 1997 storm, *J. Geophys. Res.*, *106*, 7–22, doi:10.1029/2000JA002008.
- Jordanova, V. K., A. Boonsiriset, R. M. Thorne, and Y. Dotan (2003), Ring current asymmetry from global simulations using a high-resolution electric field model, *J. Geophys. Res.*, *108*(A12), 1443, doi:10.1029/2003JA009993.
- Khazanov, G. V., K. V. Gamayunov, V. K. Jordanova, and E. N. Krivorutsky (2002), A self-consistent model of the interacting ring current ions and electromagnetic ion cyclotron waves, initial results: Waves and precipitating fluxes, *J. Geophys. Res.*, *107*(A6), 1085, doi:10.1029/2001JA000180.
- Khazanov, G. V., K. V. Gamayunov, D. L. Gallagher, and J. U. Kozyra (2006), Self-consistent model of magnetospheric ring current and propagating electromagnetic ion cyclotron waves: Waves in multi-ion magnetosphere, *J. Geophys. Res.*, *111*, A10202, doi:10.1029/2006JA011833.
- Khazanov, G. V., K. V. Gamayunov, D. L. Gallagher, and J. U. Kozyra (2007), Reply to comment by R. M. Thorne and R. B. Horne on *Khazanov et al.* [2002] and *Khazanov et al.* [2006], *J. Geophys. Res.*, *112*, A12215, doi:10.1029/2007JA012463.
- Kozyra, J. U., V. K. Jordanova, R. B. Horne, and R. M. Thorne (1997), Modeling of the contribution of electromagnetic ion cyclotron (EMIC) waves to stormtime ring current erosion, in *Magnetic Storms*, *Geophys. Monogr. Ser.*, vol. 98, edited by B. T. Tsurutani et al., pp. 187–202, AGU, Washington, D. C.
- Lyons, L. R., and R. M. Thorne (1972), Parasitic pitch angle diffusion of radiation belt particles by ion cyclotron waves, *J. Geophys. Res.*, *77*, 5608–5616, doi:10.1029/JA077i028p05608.
- Mauk, B. H., C. E. McIlwain, and R. L. McPherron (1981), Helium cyclotron resonance within the Earth's magnetosphere, *Geophys. Res. Lett.*, *8*, 103–106, doi:10.1029/GL008i001p0103.
- Meredith, N. P., R. M. Thorne, R. B. Horne, D. Summers, B. J. Fraser, and R. R. Anderson (2003), Statistical analysis of relativistic electron energies for cyclotron resonance with EMIC waves observed on CRRES, *J. Geophys. Res.*, *108*(A6), 1250, doi:10.1029/2002JA009700.
- Omura, Y., M. Ashour-Abdalla, R. Gendrin, and K. Quest (1985), Heating of thermal helium in the equatorial magnetosphere: A simulation study, *J. Geophys. Res.*, *90*, 8281–8292, doi:10.1029/JA090iA09p08281.
- Prigancová, A., and Y. I. Feldstein (1992), Magnetospheric storm dynamics in terms of energy output rate, *Planet. Space Sci.*, *40*, 581–588, doi:10.1016/0032-0633(92)90272-P.
- Roux, A., S. Perraut, J. L. Rauch, C. de Villedary, G. Kremser, A. Korth, and D. T. Young (1982), Wave-particle interactions near $\Omega_{\text{He}^+}^+$ observed on board GEOS 1 and 2: 2. Generation of ion cyclotron waves and heating of He⁺ ions, *J. Geophys. Res.*, *87*, 8174–8190, doi:10.1029/JA087iA10p08174.
- Summers, D., and R. M. Thorne (2003), Relativistic electron pitch-angle scattering by electromagnetic ion cyclotron waves during geomagnetic storms, *J. Geophys. Res.*, *108*(A4), 1143, doi:10.1029/2002JA009489.
- Thorne, R. M., and R. B. Horne (1992), The contribution of ion-cyclotron waves to electron heating and SAR-arc excitation near the storm-time plasmapause, *Geophys. Res. Lett.*, *19*, 417–420, doi:10.1029/92GL00089.
- Thorne, R. M., and R. B. Horne (1997), Modulation of electromagnetic ion cyclotron instability due to interaction with ring current O⁺ during magnetic storms, *J. Geophys. Res.*, *102*(A7), 14,155–14,163, doi:10.1029/96JA04019.
- Thorne, R. M., and C. F. Kennel (1971), Relativistic electron precipitation during magnetic storm main phase, *J. Geophys. Res.*, *76*, 4446–4453, doi:10.1029/JA076i019p04446.
- Winske, D., and N. Omidi (1993), Hybrid codes: Methods and applications, in *Computer Space Plasma Physics: Simulation Techniques and Software*, edited by H. Matsumoto and Y. Omura, pp. 103–160, Terra Sci., Tokyo.
- Winske, D., and N. Omidi (1996), A nonspecialist's guide to kinetic simulations of space plasmas, *J. Geophys. Res.*, *101*, 17,287–17,303, doi:10.1029/96JA00982.
- Winske, D., L. Yin, N. Omidi, H. Karimabadi, and K. Quest (2003), Hybrid simulation codes: Past, present and future—A Tutorial, in *Space Plasma Simulation*, *Lecture Notes Phys.*, vol. 615, edited by J. Büchner, C. T. Dum, and M. Scholer, pp. 136–165, Springer, Berlin, doi:10.1007/3-540-36530-3_8.

J. Bortnik and R. M. Thorne, Department of Atmospheric and Oceanic Sciences, University of California, Los Angeles, CA 90095-1565, USA. (jbortnik@gmail.com; rmt@atmos.ucla.edu)

N. Omidi, Solana Scientific Inc., 777 S. Pacific Coast Hwy., Ste. 208B, Solana Beach, CA 92075, USA. (omidi@solanasci.com)